ChemComm

COMMUNICATION

View Article Online
View Journal | View Issue

Cite this: *Chem. Commun.*, 2016, 52, 4191

Received 7th December 2015,
Accepted 16th February 2016

DOI: 10.1039/c5cc10063a

www.rsc.org/chemcomm

Triggering autocatalytic reaction by host–guest interactions†

Volodymyr Sashuk,* Helena Butkiewicz, Marcin Fiałkowski and Oksana Danylyuk*

The acceleration of a sequential reaction through electrostatic alteration of substrate basicity within a supramolecular host is demonstrated. In the presence of the host, the reaction, which is autocatalytic, starts much sooner and exhibits substrate size selectivity.

Remote substrate activation is a distinctive trait of enzyme catalysis.[1] Being nested in the enzyme pocket, the substrate is exposed to an electrostatic environment created by the protein residues. This entails modifying the acid–base properties (pK_a) of the bound substrate, and in consequence, facilitates its hydrolysis. In some cases, the magnitude of the apparent pK_a shift even reaches up to five units.[2] It has long been endeavored to reproduce similar (biomimetic) action in synthetic hosts that are reminiscent of enzyme cavities.[3–16] However, this has proved very challenging, as it requires a host that would meet several criteria, especially the capability of stabilizing the charged transition state. Raymond and co-workers have recently presented the first successful demonstration of electrostatic catalysis based on ion–ion interactions by using a tetrahedral metal cluster which consists of a hydrophobic cavity and negatively charged vertices.[17–24] It was found that the complex alters the pK_a of the encapsulated guest to the extent that it enables acid hydrolysis at basic pH.[17,21] Further research, in particular by the Nau group, has revealed that a similar electrostatic action *via* ion–dipole interactions is also possible in cucurbit[*n*]uril (**CB**) hosts, which are a family of barrel-shaped macrocycles[25–38] composed of a hydrophobic cavity and an electronegative carbonyl-fringed rim. Like the metal cluster, the **CB** host was shown to promote hydrolysis reactions *via* Coulombic stabilization of the protonated substrate.[39–41] Most recently, the stabilization of positively charged species in transition state through ion–π interactions has also been suggested for resorcin[4]arene capsules.[42–46] Being intrigued by these results, we pursued the studies to broaden the scope of electrostatic catalysis towards multistep chemical transformations.

Herein, we report a sequential azo coupling-type reaction promoted by electrostatic **CB** host–guest interactions. Azo coupling is an important chemical process used in industry for the production of azo dyes.[47] Apart from the textile-dyeing industry, azo compounds are also used as pH indicators and molecular photoswitches.[48,49] The coupling reaction usually occurs between an aromatic compound and diazonium salt, which has to be generated *in situ* due to high instability. In this respect, triazene is a robust substitute for the diazonium salt.[50] We found that triazene reacts with an electron-rich arene in the presence of cucurbit[6]uril (**CB6**) affording an azo dye. Since the background reaction is negligible in the timescale of the catalytic event, we may talk here about triggering the reaction.

In our study, we employed berenil ($\mathbf{S_1}$), a commercially available triazene which is an anti-infective drug (Fig. 1a). Resorcinol ($\mathbf{S_2}$) served as the aromatic partner in the reaction. In a typical experiment, a stoichiometric mixture of $\mathbf{S_1}$, $\mathbf{S_2}$, and **CB6** were suspended by agitation in heavy water and kept at room temperature. The experiment was carried out at near neutral pD without buffering. During the experiment, the pD of the suspension changed from 7.4 to 4.2 and the azo dye product ($\mathbf{P_3}$) precipitated as an orange solid. The process was monitored by ^{1}H NMR spectroscopy following the formation of 4-aminobenzamidine ($\mathbf{P_1}$), which is another product of the reaction. According to the NMR data, the reaction was complete within two weeks, whereas only traces (<1 mol%) of $\mathbf{P_1}$ were detected in the control experiment performed without **CB6**. The azo dye product $\mathbf{P_3}$ was isolated from the **CB6** precipitate by addition of calcium chloride followed by filtration and recrystallization from hydrochloric acid solution. X-ray diffraction of the isolated orange crystals, along with NMR and MS analysis, confirmed the expected structure of the azo dye (Fig. 1c). The azo product $\mathbf{P_3}$ was also crystallized as the inclusion complex with **CB6** upon the acidification of the crude reaction mixture (Fig. 1d).

Institute of Physical Chemistry, Polish Academy of Sciences, Kasprzaka 44/52, 01-224 Warsaw, Poland. E-mail: vsashuk@ichf.edu.pl, odanylyuk@ichf.edu.pl

† Electronic supplementary information (ESI) available: Synthetic procedures, spectroscopic data, kinetic model. CCDC 1440778–1440781. For ESI and crystallographic data in CIF or other electronic format see DOI: 10.1039/c5cc10063a

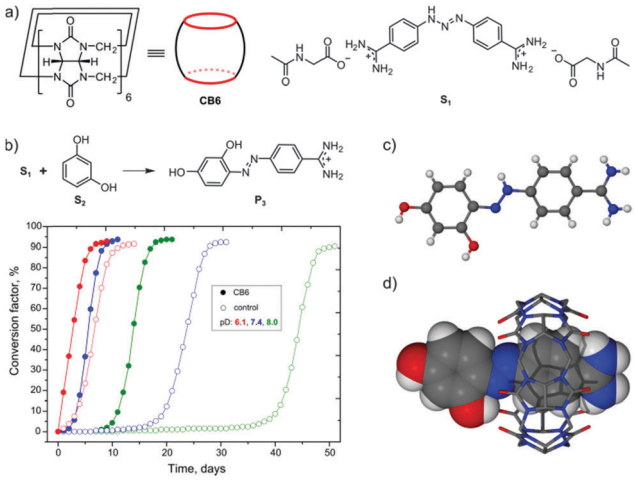

Fig. 1 (a) Chemical structure of cucurbit[6]uril (**CB6**) and berenil (**S_1**); (b) reaction scheme and plots of the time dependence of the conversion factor for azo coupling between **S_1** and resorcinol (**S_2**) in the presence and absence of **CB6** for different values of pD; (c) X-ray structure of azo dye product **P_3**; (d) X-ray structure of inclusion complex between **CB6** and **P_3**.

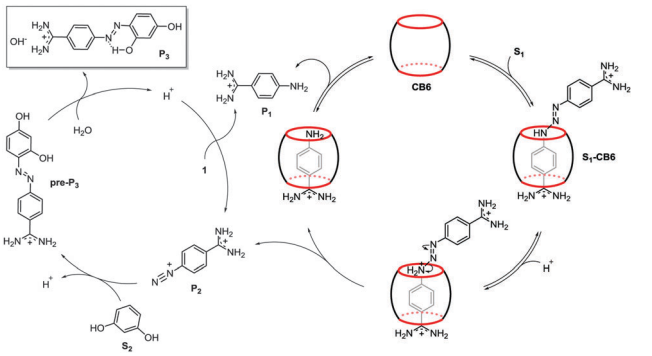

Fig. 2 Plausible mechanism of **CB6**-catalyzed sequential azo coupling-type reaction. The first step of the reaction is the acid hydrolysis of **S_1**, promoted by electrostatic action of **CB6**. In the next step, the generated diazonium intermediate **P_2** reacts with **S_2** to yield azo compound **pre-P_3**. The compound **pre-P_3** is next transformed to final azo product **P_3** with loss of a proton, which acidifies the reaction mixture, accelerating the hydrolysis of **S_1**, and consequently the overall reaction.

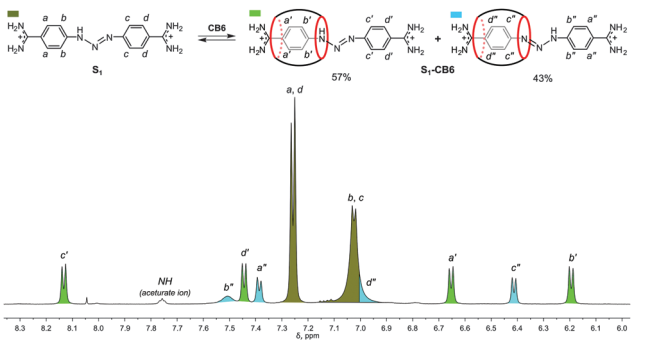

Fig. 3 Partial ^{1}H NMR spectrum of equimolar mixture of **S_1** and **CB6** in D_2O, 277 K. The tautomeric ratio was calculated by the integration of the corresponding peaks.

To monitor the progress of the reaction, we calculated the quantity $\gamma = [\mathbf{P_1}]/([\mathbf{S_2}] + [\mathbf{P_1}]) \times 100\%$. In the following, we refer to the quantity γ as the conversion factor. The time dependence of the conversion factor for the coupling reaction at different pD values is plotted in Fig. 1b. The coupling reaction is pH-sensitive, exhibiting autocatalytic behavior in nearly neutral solutions. The involvement of **CB6** in the process is manifested by a shorter induction period as well as a steeper curve during the acceleration phase when compared with the control experiment. The most spectacular effect of the action of **CB6** was observed in basic solution, with the lag phase being reduced by one month.

The plausible mechanism of the reaction is depicted in Fig. 2. In the first step, the triazene molecule **S_1** is encapsulated by the **CB** host. The encapsulation is facilitated by the template effect of the positively charged amidinium terminus, which interacts electrostatically with the electronegative **CB** rim. The formation of the host–guest species is clearly seen in the NMR spectrum after mixing the reactants (Fig. S1, ESI†). The proton resonances of the aromatic ring placed inside the **CB** cavity are shifted upfield, while the signals of the aromatic protons positioned outside the cavity move toward the downfield region. Low-temperature NMR measurements of the **S_1–CB6** mixture revealed that the observed shifts are attributed to the formation of two host–guest **CB6** complexes (**S_1–CB6**) comprising "frozen" tautomeric forms of the thermodynamically stable *trans* isomer[51] of **S_1** (Fig. 3 and Fig. S6–S8, ESI†). The weak differentiation of the resonance structures of **S_1** upon the encapsulation indicates that either the NH group of the triazene moiety in both tautomers is in close proximity to the carbonyl portals of the **CB** rim or the hydrogen bonding is not a dominant force in the binding event, which would be consistent with previous reports.[28] Hence, it is not clear which tautomer is a reaction intermediate. A possible reaction scenario involving the major tautomer is shown in Fig. 2. The enhanced electron density at the **CB** rim increases the basicity of the encapsulated substrate, rendering the triazene moiety susceptible to protonation and subsequent rupture with formation of 4-amidinophenyldiazonium (**P_2**). Despite high **CB6** loading, the cleavage reaction was triggered by catalytic amounts of the **S_1–CB6** complex (*ca.* 15 mol%) formed at pre-equilibrium. Importantly, the employment of sub-stoichiometric amounts of **CB6** (20 mol%) did not affect the reaction rate significantly as the initial amount of the inclusion complex formed was about 5 mol% (Fig. S8, ESI†). As the reaction progresses, the vast fraction of the **S_1–CB6** complex is quickly consumed and not further replenished by virtue of competitive binding of **P_1** to **CB6**. In the next step, the diazonium cation **P_2** reacts with **S_2** *via* electrophilic substitution to give azo compound **pre-P_3**. The substitution reaction is favored by alkaline pH, though also remains feasible under acidic conditions.[52] With the acidification of the reaction mixture, caused by the hydrolysis of **pre-P_3** to insoluble **P_3**, the hydrolysis of **S_1**, and consequently the overall reaction, accelerates. Although the **S_1–CB6** complex was not detected by NMR at this stage, the hydrolysis of **S_1**, as judged from the kinetic slopes, does take place inside the macrocycle cavity. The plot showing the pD of the reaction mixture as a function of time is shown in Fig. S10 (ESI†). The product **P_3** precipitates probably due to intramolecular hydrogen bonding between the azo bond and nearby hydroxyl group.[52]

Of note, under strongly acidic conditions the hydrogen bond vanishes at the expense of protonation of the azo dye bond (Fig. 1c).

To verify the proposed mechanism, we modeled the **CB6**-catalyzed sequential reaction using the following set of two rate equations:

$$\mathbf{S_1} + D_2O + D^+ \xrightarrow{k_1} \mathbf{P_1} + \mathbf{P_2} + D^+ \qquad \text{(i)}$$

and

$$\mathbf{S_2} + \mathbf{P_2} \xrightarrow{k_2} \mathbf{P_3} + D^+. \qquad \text{(ii)}$$

The first equation is the hydrolysis of $\mathbf{S_1}$. The second reaction describes the azo coupling step. The acid specific hydrolysis rate constant, k_H, in eqn (i) had the form $k_H = k_1^{n,c}[D^+]$, where the superscripts n and c refer, respectively, to the neutral (control) and **CB6**-catalyzed reaction. The constant term in k_1 was set equal to zero to account for the fact that in all experimental conditions the induction periods (the lag phases) were observed. The eqn (i) and (ii) were solved numerically and the conversion factor, γ, was calculated as a function of time for pD = 8.0, 7.4, and 6.1. The rate constants k_1^n, k_1^c, and k_2 were determined by least-square fitting to the experimental values of γ (see ESI† for details). Numerical analysis of the rate equations showed the increase of both rate constants k_1^n and k_1^c with the decrease of pD. This tendency is in line with results reported recently for the hydrolysis of $\mathbf{S_1}$.[53] As expected, we also observed a substantial decrease of the rate constant k_2 with increasing acidity of the system. To quantify the catalytic effect of **CB6**, for each value of pD we calculated the acceleration factor defined as the ratio k_1^c/k_1^n. Based on the results of the numerical analysis of the rate constants, we obtained the acceleration factors 3.24, 5.47, and 5.12 for pD equal to 8.0, 7.4, and 6.1, respectively.

When $\mathbf{S_2}$ was substituted by phenol ($\mathbf{S_3}$), the coupling reaction significantly slowed down (Fig. 4a). Since the resulting azo product ($\mathbf{P_4}$, the X-ray structure is shown in Fig. 4b) lacks the intramolecular hydrogen bonding, the equilibrium does not shift towards its hydrolysis. As a result, the pD of the reaction mixture changed from 7.2 to 6.4, and no autocatalysis was observed. The slow reaction rate surprisingly also stems from the competitive binding of $\mathbf{S_3}$, which displaces encapsulated $\mathbf{S_1}$ from the **CB** cavity. It is noteworthy that this kind of competition was not observed for $\mathbf{S_2}$, suggesting the size selectivity of the **CB6** ring. During the first day of the experiment, the content of $\mathbf{S_1}$–**CB6** complex in the solution dropped below 0.5 mol%. The process is supposedly precipitation-driven considering the higher affinity of cationic guests toward the **CB** host. The precipitation of phenol–**CB6** ($\mathbf{S_3}$–**CB6**) complex can be delayed by addition of calcium chloride. In this case, the process of inclusion was observed through upfield shifts of the phenolic NMR signals followed by slow crystallization of $\mathbf{S_3}$–**CB6**, whose structure was further corroborated by single crystal X-ray analysis (Fig. 4c).

To unequivocally prove the catalytic properties of **CB6**, the coupling reaction between $\mathbf{S_1}$ and $\mathbf{S_2}$ was conducted with a stoichiometric admixture of $\mathbf{S_3}$. As expected, the reaction was greatly inhibited due to competitive binding of $\mathbf{S_3}$ for the **CB** cavity, which confirms nicely the action of **CB6** as a catalyst (Fig. 5).

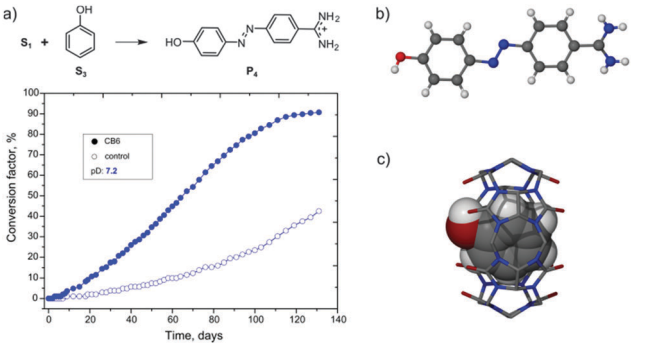

Fig. 4 (a) Reaction scheme and plots of the time dependence of the conversion factor for azo coupling between $\mathbf{S_1}$ and phenol ($\mathbf{S_3}$) in the presence and absence of **CB6**; (b) X-ray structure of azo dye product $\mathbf{P_4}$; (c) X-ray structure of inclusion complex between $\mathbf{S_3}$ and **CB6**.

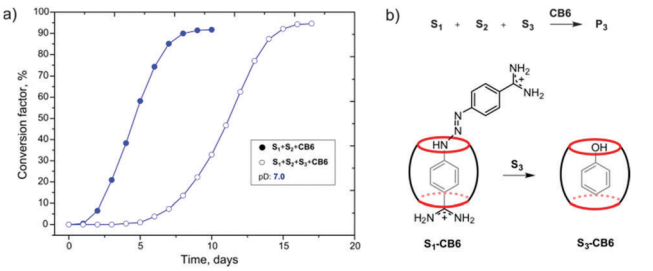

Fig. 5 (a) Plots of the time dependence of the conversion factor for **CB6**-catalyzed azo coupling between $\mathbf{S_1}$ and $\mathbf{S_2}$ in the presence and absence of $\mathbf{S_3}$; (b) schematic representation of competitive binding of $\mathbf{S_3}$ to **CB6** in the reaction between $\mathbf{S_1}$ and $\mathbf{S_2}$ in the presence of $\mathbf{S_3}$.

The reaction inhibition was also observed in the presence of 1,5-pentanediamine (cadaverine), which forms a strong complex with **CB6** (Fig. S10, ESI†).

In summary, we designed a two-step azo coupling-type reaction induced by host–guest interactions. A peculiar feature of the reaction is that the first step is acid-catalyzed, whereas the next step prefers non-acidic conditions. Normally, if the reaction is performed in acidic medium, the fast hydrolysis step is followed by slow electrophilic substitution, and *vice versa*, the reaction is extremely sluggish in neutral and alkaline solutions. The use of the **CB6** host as a catalyst facilitates the acid hydrolysis, and consequently the overall reaction at basic pH through the electrostatic enhancement of substrate basicity. Accordingly, the reaction, being autocatalytic, begins much earlier, *i.e.*, is triggered by **CB6**. The presented concept is of great importance for the development of chemical transformations involving discrete reaction steps occurring at different pH values. Furthermore, this strategy, given the substrate size selectivity, may be applicable for performing acid-catalyzed reactions on selected functional groups in the presence of other functionalities sensitive to acidic conditions.

The project was supported by the Polish Ministry of Science and Higher Education (grant Iuventus Plus Nr IP2012 008272).

Notes and references

1 A. Warshel, P. K. Sharma, M. Kato, Y. Xiang, H. Liu and M. H. M. Olsson, *Chem. Rev.*, 2006, **106**, 3210–3235.

2 F. H. Westheimer, *Tetrahedron*, 1995, **51**, 3–20.
3 M. Raynal, P. Ballester, A. Vidal-Ferran and P. W. N. M. van Leeuwen, *Chem. Soc. Rev.*, 2014, **43**, 1734–1787.
4 J. Meeuwissen and J. N. H. Reek, *Nat. Chem.*, 2010, **2**, 615–621.
5 M. Yoshizawa, J. K. Klosterman and M. Fujita, *Angew. Chem., Int. Ed.*, 2009, **48**, 3418–3438.
6 S. H. A. M. Leenders, R. Gramage-Doria, B. de Bruin and J. N. H. Reek, *Chem. Soc. Rev.*, 2015, **44**, 433–448.
7 T. S. Koblenz, J. Wassenaar and J. N. H. Reek, *Chem. Soc. Rev.*, 2008, **37**, 247–262.
8 C. J. Walter and J. K. M. Sanders, *Angew. Chem., Int. Ed. Engl.*, 1995, **34**, 217–219.
9 J. Kang and J. Rebek, *Nature*, 1997, **385**, 50–52.
10 M. Yoshizawa, M. Tamura and M. Fujita, *Science*, 2006, **312**, 251–254.
11 S. R. Shenoy, F. R. Pinacho Crisóstomo, T. Iwasawa and J. Rebek, *J. Am. Chem. Soc.*, 2008, **130**, 5658–5659.
12 P. Thordarson, E. J. A. Bijsterveld, A. E. Rowan and R. J. M. Nolte, *Nature*, 2003, **424**, 915–918.
13 E. Anslyn and R. Breslow, *J. Am. Chem. Soc.*, 1989, **111**, 5972–5973.
14 F. Ortega-Caballero, C. Rousseau, B. Christensen, T. E. Petersen and M. Bols, *J. Am. Chem. Soc.*, 2005, **127**, 3238–3239.
15 M. J. Wiester, P. A. Ulmann and C. A. Mirkin, *Angew. Chem., Int. Ed.*, 2011, **50**, 114–137.
16 A. G. Salles, S. Zarra, R. M. Turner and J. R. Nitschke, *J. Am. Chem. Soc.*, 2013, **135**, 19143–19146.
17 M. D. Pluth, R. G. Bergman and K. N. Raymond, *Science*, 2007, **316**, 85–88.
18 W. M. Hart-Cooper, K. N. Clary, F. D. Toste, R. G. Bergman and K. N. Raymond, *J. Am. Chem. Soc.*, 2012, **134**, 17873–17876.
19 C. J. Hastings, M. P. Backlund, R. G. Bergman and K. N. Raymond, *Angew. Chem., Int. Ed.*, 2011, **50**, 10570–10573.
20 C. J. Hastings, M. D. Pluth, R. G. Bergman and K. N. Raymond, *J. Am. Chem. Soc.*, 2010, **132**, 6938–6940.
21 M. D. Pluth, R. G. Bergman and K. N. Raymond, *J. Am. Chem. Soc.*, 2008, **130**, 11423–11429.
22 C. Zhao, F. D. Toste, K. N. Raymond and R. G. Bergman, *J. Am. Chem. Soc.*, 2014, **136**, 14409–14412.
23 C. Zhao, Q.-F. Sun, W. M. Hart-Cooper, A. G. DiPasquale, F. D. Toste, R. G. Bergman and K. N. Raymond, *J. Am. Chem. Soc.*, 2013, **135**, 18802–18805.
24 Z. J. Wang, K. N. Clary, R. G. Bergman, K. N. Raymond and F. D. Toste, *Nat. Chem.*, 2013, **5**, 100–103.
25 J. W. Lee, S. Samal, N. Selvapalam, H.-J. Kim and K. Kim, *Acc. Chem. Res.*, 2003, **36**, 621–630.
26 J. Lagona, P. Mukhopadhyay, S. Chakrabarti and L. Isaacs, *Angew. Chem., Int. Ed.*, 2005, **44**, 4844–4870.
27 B. C. Pemberton, R. Raghunathan, S. Volla and J. Sivaguru, *Chem. – Eur. J.*, 2012, **18**, 12178–12190.
28 K. I. Assaf and W. M. Nau, *Chem. Soc. Rev.*, 2015, **44**, 394–418.
29 A. L. Koner, C. Márquez, M. H. Dickman and W. M. Nau, *Angew. Chem., Int. Ed.*, 2011, **50**, 545–548.
30 X. Lu and E. Masson, *Org. Lett.*, 2010, **12**, 2310–2313.
31 H. Cong, Z. Tao, S. F. Xue and Q. J. Zhu, *Curr. Org. Chem.*, 2011, **15**, 86–95.
32 L. Zheng, S. Sonzini, M. Ambarwati, E. Rosta, O. A. Scherman and A. Herrmann, *Angew. Chem., Int. Ed.*, 2015, **54**, 13007–13011.
33 W. L. Mock, T. A. Irra, J. P. Wepsiec and M. Adhya, *J. Org. Chem.*, 1989, **54**, 5302–5308.
34 S. Y. Jon, Y. H. Ko, S. H. Park, H.-J. Kim and K. Kim, *Chem. Commun.*, 2001, 1938–1939.
35 B. C. Pemberton, N. Barooah, D. K. Srivatsava and J. Sivaguru, *Chem. Commun.*, 2010, **46**, 225–227.
36 B. C. Pemberton, R. K. Singh, A. C. Johnson, S. Jockusch, J. P. Da Silva, A. Ugrinov, N. J. Turro, D. K. Srivastava and J. Sivaguru, *Chem. Commun.*, 2011, **47**, 6323–6325.
37 C. Yang, T. Mori, Y. Origane, Y. H. Ko, N. Selvapalam, K. Kim and Y. Inoue, *J. Am. Chem. Soc.*, 2008, **130**, 8574–8575.
38 S. J. Barrow, S. Kasera, M. J. Rowland, J. del Barrio and O. A. Scherman, *Chem. Rev.*, 2015, **115**, 12320–12406.
39 N. i. Saleh, A. L. Koner and W. M. Nau, *Angew. Chem., Int. Ed.*, 2008, **47**, 5398–5401.
40 C. Klöck, R. N. Dsouza and W. M. Nau, *Org. Lett.*, 2009, **11**, 2595–2598.
41 N. Basilio, L. García-Río, J. A. Moreira and M. Pessêgo, *J. Org. Chem.*, 2010, **75**, 848–855.
42 A. Cavarzan, A. Scarso, P. Sgarbossa, G. Strukul and J. N. H. Reek, *J. Am. Chem. Soc.*, 2011, **133**, 2848–2851.
43 G. Bianchini, G. L. Sorella, N. Canever, A. Scarso and G. Strukul, *Chem. Commun.*, 2013, **49**, 5322–5324.
44 Q. Zhang and K. Tiefenbacher, *J. Am. Chem. Soc.*, 2013, **135**, 16213–16219.
45 L. Catti and K. Tiefenbacher, *Chem. Commun.*, 2015, **51**, 892–894.
46 Q. Zhang and K. Tiefenbacher, *Nat. Chem.*, 2015, **7**, 197–202.
47 K. Hunger, P. Mischke and W. Rieper, *Ullmann's Encyclopedia of Industrial Chemistry*, Wiley-VCH Verlag GmbH & Co. KGaA, 2000.
48 A. A. Beharry and G. A. Woolley, *Chem. Soc. Rev.*, 2011, **40**, 4422–4437.
49 R. Klajn, *Pure Appl. Chem.*, 2010, **82**, 2247–2279.
50 S. Bräse, *Acc. Chem. Res.*, 2004, **37**, 805–816.
51 M. Barra and N. Chen, *J. Org. Chem.*, 2000, **65**, 5739–5744.
52 O. Macháčková, V. Štěrba and K. Valter, *Collect. Czech. Chem. Commun.*, 1972, **37**, 1851–1860.
53 M. Campbell, R. J. Prankerd, A. S. Davie and W. N. Charman, *J. Pharm. Pharmacol.*, 2004, **56**, 1327–1332.